Miner Deposita (2013) 48:295–311
DOI 10.1007/s00126-012-0425-4

ARTICLE

Silver-rich telluride mineralization at Mount Charlotte and Au–Ag zonation in the giant Golden Mile deposit, Kalgoorlie, Western Australia

Andreas G. Mueller · Janet R. Muhling

Received: 13 December 2011 / Accepted: 22 May 2012 / Published online: 6 July 2012

Abstract The gold deposits at Kalgoorlie in the 2.7-Ga Eastern Goldfields Province of the Yilgarn Craton, Western Australia, occur adjacent to the D2 Golden Mile Fault over a strike of 8 km within a district-scale zone marked by porphyry dykes and chloritic alteration. The late Golden Pike Fault separates the older (D2) shear zone system of the Golden Mile (1,500 t Au) in the southeast from the younger (D4) quartz vein stockworks at Mt Charlotte (126 t Au) in the northwest. Both deposits occur in the Golden Mile Dolerite sill and display inner sericite–ankerite alteration and early-stage gold–pyrite mineralization replacing the wall rocks. Late-stage tellurides account for 20 % of the total gold in the first, but for <1 % in the second deposit. In the Golden Mile, the main telluride assemblage is coloradoite+native gold (898–972 fine)+calaverite+petzite± krennerite. Telluride-rich ore (>30 g/t Au) is characterized by Au/Ag=2.54 and As/Sb=2.6–30, the latter ratio caused by arsenical pyrite. Golden Mile-type D2 lodes occur northwest of the Golden Pike Fault, but the Hidden Secret orebody, the only telluride bonanza mined (10,815 t at 44 g/t Au), was unusually rich in silver (Au/Ag=0.12–0.35) due to abundant hessite. We describe another array of silver-rich D2 shear zones which are part of the Golden Mile Fault exposed on the Mt Charlotte mine 22 level. They are filled with crack-seal and pinch-and-swell quartz–carbonate veins and are surrounded by early-stage pyrite+pyrrhotite disseminated in a sericite–ankerite zone more than 6 m wide. Gold grade (0.5–0.8 g/t) varies little across the zone, but Au/Ag (0.37–2.40) and As/Sb (1.54–13.9) increase away from the veins. Late-stage telluride mineralization (23 g/t Au) sampled in one vein has a much lower Au/Ag (0.13) and As/Sb (0.48) and comprises scheelite, pyrite, native gold (830–854 fine), hessite, and minor pyrrhotite, altaite, bournonite, and boulangerite. Assuming 250–300 °C, gold–hessite compositions indicate a fluid log f_{Te2} of −11.5 to −10, values well below the stability of calaverite. The absence of calaverite and the dominance of hessite in the D2 lodes of the Mt Charlotte area point to a kilometer-scale mineral and Au/Ag zonation along the Golden Mile master fault, which is attributed to a lateral decrease in peak tellurium fugacity of the late-stage hydrothermal fluid. The As/Sb ratio may be similarly zoned to lower values at the periphery. The D4 gold–quartz veins constituting the Mt Charlotte orebodies represent a younger hydrothermal system, which did not contribute to metal zonation in the older one.

Keywords Archaean · Golden Mile · Gold · Silver · Tellurides · Au–Ag zonation

Editorial handling: B. Lehmann

A. G. Mueller (✉)
12a Belgrave Street,
Maylands, WA 6051, Australia
e-mail: andreasm@iinet.net.au

J. R. Muhling
Centre for Microscopy, Characterisation and Analysis M010,
The University of Western Australia,
35 Stirling Highway,
Crawley, WA 6009, Australia

Introduction

Recent studies have outlined kilometer-scale mineral and metal zonation along faults in intrusion-centered Au–Ag–Cu mining districts, emphasizing the importance of pattern recognition in targeting exploration (e.g., Johnson 2000; Chang et al. 2011). In the Kalgoorlie district, located in the Eastern Goldfields Province of the Archaean Yilgarn Craton, porphyry dykes and gold mineralization within

and adjacent to the Golden Mile Fault are coincident over a strike length of 8 km. The two main deposits, the Golden Mile (1,500 t Au produced) in the southeast and Mt Charlotte (126 t Au) in the northwest, are about 3 km apart (Fig. 1). Both are commonly interpreted as "orogenic deposits" unrelated to magmatic processes (e.g., Groves et al. 1998). However, they differ markedly in ore mineralogy. In the Golden Mile shear zone system, most gold occurs enclosed in early-stage arsenical pyrite, while late-stage Au–Ag tellurides contribute 20% of the total. In the quartz vein stockworks at Mt Charlotte, gold occurs attached to arsenic-poor pyrite and tellurides contribute <1% (Clout et al. 1990).

Despite the early discovery of the telluride ore in the Hidden Secret Mine close to Mt Charlotte (Simpson 1912), the scarcity of tellurides in the bulk-minable vein stockworks led to the assumption that deposits in the northwest Kalgoorlie district are unrelated to those in the Golden Mile (e.g., Travis et al. 1971). This view was reinforced by the silver-rich nature of the Hidden Secret bonanza (10,815 metric tons at 44.25 g/t Au; Au/Ag=0.35; Feldtmann 1916), which is at odds with the lower silver content of the high-grade telluride ore in the Golden Mile (average Au/Ag=2.54).

Shear zone-hosted lodes in the Mt Charlotte area have contributed little (18.5 t Au) to the total gold production of the district and have not been subject to recent geochemical or mineralogical studies. We describe the structure and mineralogy of Golden Mile-type shear veins exposed on the 22 level of the Mt Charlotte Mine, the second local occurrence of a silver-rich telluride mineralization. We provide electron microprobe analyses of gold, tellurides, and Pb–Sb sulfosalts complimentary to microscopic data from the Hidden Secret Lode (Simpson 1912; Stillwell 1931). We use these mineral assemblages and compositions to constrain the tellurium fugacity of the hydrothermal fluid, and we present trace element analyses and ratios suggesting large-scale telluride and Au–Ag zonation in the Golden Mile deposit.

Regional geology

The Eastern Goldfields Superterrane or Province (EGP) of the Archaean Yilgarn Craton (inset map in Fig. 1) is characterized by a 2.73- to 2.65-Ga greenstone succession setting it apart from the foreland to the west, where most greenstone belts are 3.0 Ga old. Subordinate 2.8-Ga greenstones occur in both the EGP and its foreland, suggesting that the province represents a continental margin orogen deeply eroded to the granite batholith level (e.g., Nelson 1997; Mueller and McNaughton 2000; Cassidy et al. 2006). The regional geology of the Kalgoorlie area, in particular the structure of the gold-rich Boulder-Lefroy–Golden Mile fault system, and the petrogenesis of high-Mg calc-alkaline intrusions emplaced along it are discussed in Swager et al. (1995) and Mueller (2007). The nature and time relations of structures in the Kalgoorlie district are described in Keats (1987), Mueller et al. (1988), and Clout et al. (1990). The part of the district southeast of the Golden Pike Fault is called "the Golden Mile" (e.g., Woodall 1965), while the part northwest of this fault is informally referred to as the Mt Charlotte area (Fig. 1). Mount Charlotte is a prominent hill close to the mine of the same name, and the datum on its summit at 421.2 m above mean sea level is the zero reference level for all mines in the district.

Greenstone belt stratigraphy

The greenschist facies stratigraphic succession at Kalgoorlie comprises submarine volcanic rocks of the Kalgoorlie Group (Swager et al. 1995) and carbonaceous siltstones, volcaniclastic greywackes, and polymictic conglomerates of the Lower and Upper Black Flag Group (Squire et al. 2010). Ultramafic flows of the Kambalda Komatiite, Middle Kalgoorlie Group, are 2,708±7 Ma old (U–Pb zircon; Nelson 1997). The Williamstown gabbro sill separating the Devon Consols high-Mg and Paringa tholeiitic pillow basalts is dated at 2,696±5 Ma (U–Pb zircon; Fletcher et al. 2001) and the Golden Mile Dolerite (GMD) at the base of the Black Flag greywacke at 2,680±9 Ma (Pb–Pb zirconolite; Rasmussen et al. 2009). The tholeiitic GMD sill, the main host rock to gold, is 600–750 m thick and subdivided into ten petrographic units traced over a strike of 13 km. Units 1 and 10 are variolitic and represent the lower and upper chilled margins formed together with units 2–5 and 9 by in situ differentiation of the initial magma pulse. The high-iron central units 6–8, enriched in titanomagnetite and ilmenite, are considered part of a second pulse. The GMD sill is metamorphosed to an actinolite–albite–epidote assemblage replaced by hydrothermal chlorite+calcite in a district-scale zone centered on the Golden Mile Fault (Travis et al. 1971).

D1 and D2 structures

The earliest structures are upright NW-striking D1 folds represented by the Kalgoorlie and Boulder anticlines and by the Kalgoorlie syncline (Woodall 1965). The folds are displaced by the Boulder-Lefroy and Golden Mile sinistral strike-slip faults (D2), the latter coincident with a narrow wedge of Black Flag greywacke marking the core of the Kalgoorlie syncline (Fig. 1). The main movement plane is at the northeast contact of this wedge, but the greywacke is altered and sheared throughout. The Golden Mile Fault dips 80–85° SW and controls two geometric arrays of mineralized D2 shear zones

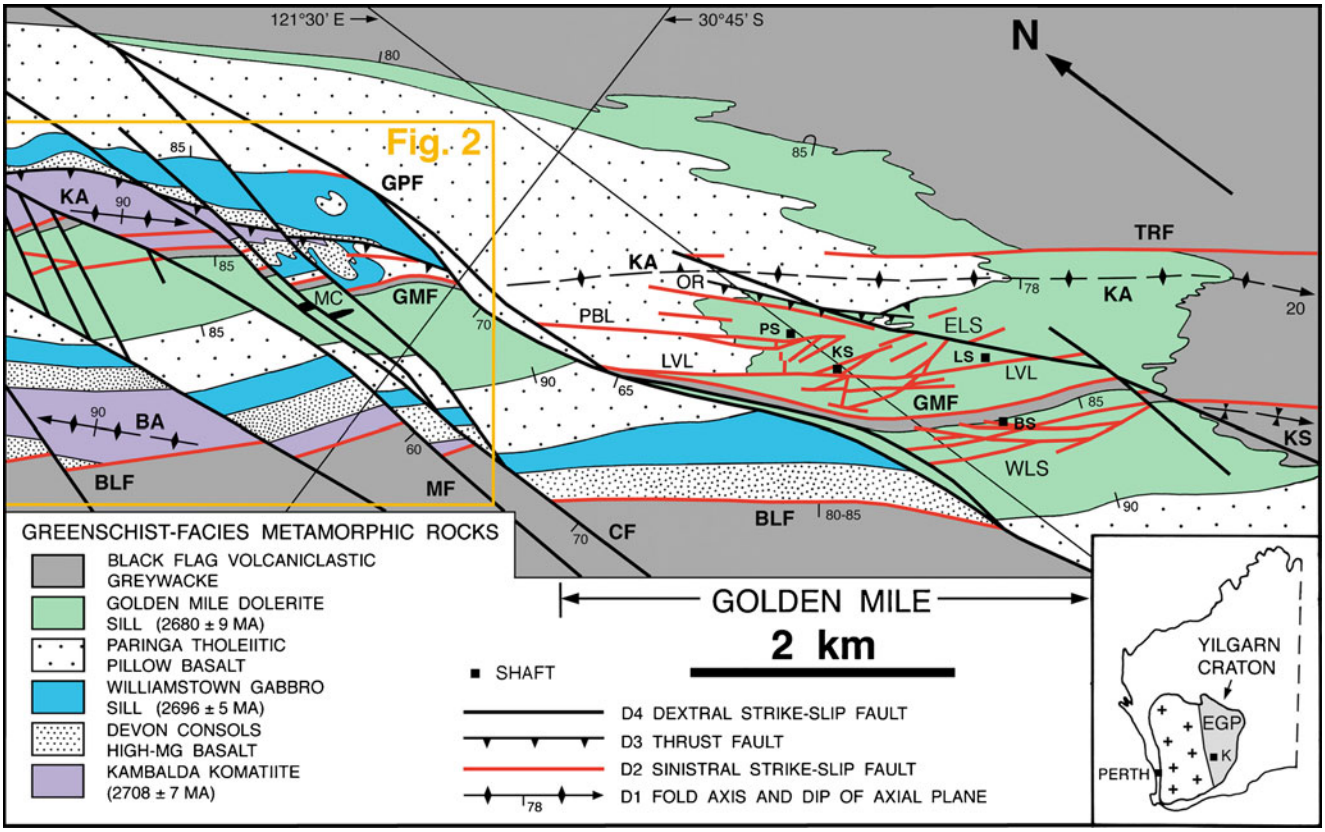

Fig. 1 Geologic map of the Kalgoorlie mining district (modified from Woodall 1965). The grid coordinates are the latitude and longitude. Upright folds (*D1*) such as the Kalgoorlie anticline (*KA*), Kalgoorlie syncline (*KS*), and Boulder anticline (*BA*) are displaced by the Boulder-Lefroy (*BLF*), Golden Mile (*GMF*), and Trafalgar (*TRF*) sinistral strike-slip faults (*D2*). The Golden Mile master fault controls shear zones subdivided into the western (*WLS*) and eastern lode systems (*ELS*), which include the D2 Lake View Lode (*LVL*), the D2 Paringa B lode (*PBL*), and the D3 Oroya Lodes (*OR*). Late dextral D4 shear zones such as the Golden Pike (*GPF*) and Charlotte Faults (*CF*) control the gold quartz vein orebodies of the Mt Charlotte mine (*MC*). Note the locations of Fig. 2 and of the Paringa South (*PS*), Kalgurli (*KS*), Lake View Main (*LS*), and Great Boulder Main (*BS*) shafts. The *inset* map of Western Australia shows the Eastern Goldfields Province (*EGP*) in the Archaean Yilgarn Craton, and the towns of Perth and Kalgoorlie (*K*)

(Mueller et al. 1988), termed the western and eastern lode systems (Woodall 1965). The eastern lodes are persistent along strike and include the Lake View Main Lode (3.5 km) and the Paringa B Lode (2 km). The western lodes are persistent to depth and include the No. 4 Lode mined to 1.2 km below the surface (Travis et al. 1971). Total ore production from the Golden Mile amounts to 106 Mt at 11.3 g/t Au underground plus 118 Mt at 2.1 g/t Au open pit (1893–2002). In the Mt Charlotte area, D2 lodes occur within and adjacent to the Golden Mile master fault (Fig. 2). Most were mined within the oxide zone, and the Hannan's North Lode is the only one recording significant underground production (0.591 Mt at 14.46 g/t Au, 1893–1952).

The schists of the Golden Mile Fault enclose numerous altered but un-metamorphosed hornblende–plagioclase porphyry dykes, and the adjacent shear zones both contain and offset dykes dated at 2,674±6 to 2,669±6 Ma (U–Pb zircon). Fuchsites from D2 lodes in the Mt Charlotte area record Ar–Ar ages of 2,653±7 and 2,654±7 Ma (Kent and McDougall 1995; Vielreicher et al. 2010). Reversely discordant zircons from a chlorite-altered lamprophyre dyke provide a minimum age of 2,642±6 Ma for mineralization in the Golden Mile (McNaughton et al. 2005).

D3 and D4 structures

Renewed compression after sinistral strike-slip faulting caused the development of D3 thrusts. In the Golden Mile, barren D3 faults displace the steeply dipping D2 lodes of the western system (Stillwell 1929). However, the reverse Oroya shear zones of the eastern system, located at the SW-dipping contact Paringa Basalt/GMD (Fig. 1), are mineralized and control a 1.1-km-long, pipe-shaped shoot set apart from all other lodes by its shallow plunge. In the Mt Charlotte Mine, two barren D3 thrusts—termed Neptune and Flanagan—are exposed in the underground workings. Both strike N25–30° W, dip 50–55° SW, and record reverse movements of 40 and 150 m, respectively. The Flanagan Fault thins stratigraphic units at the northeast limb of the Kalgoorlie anticline (Keats 1987).

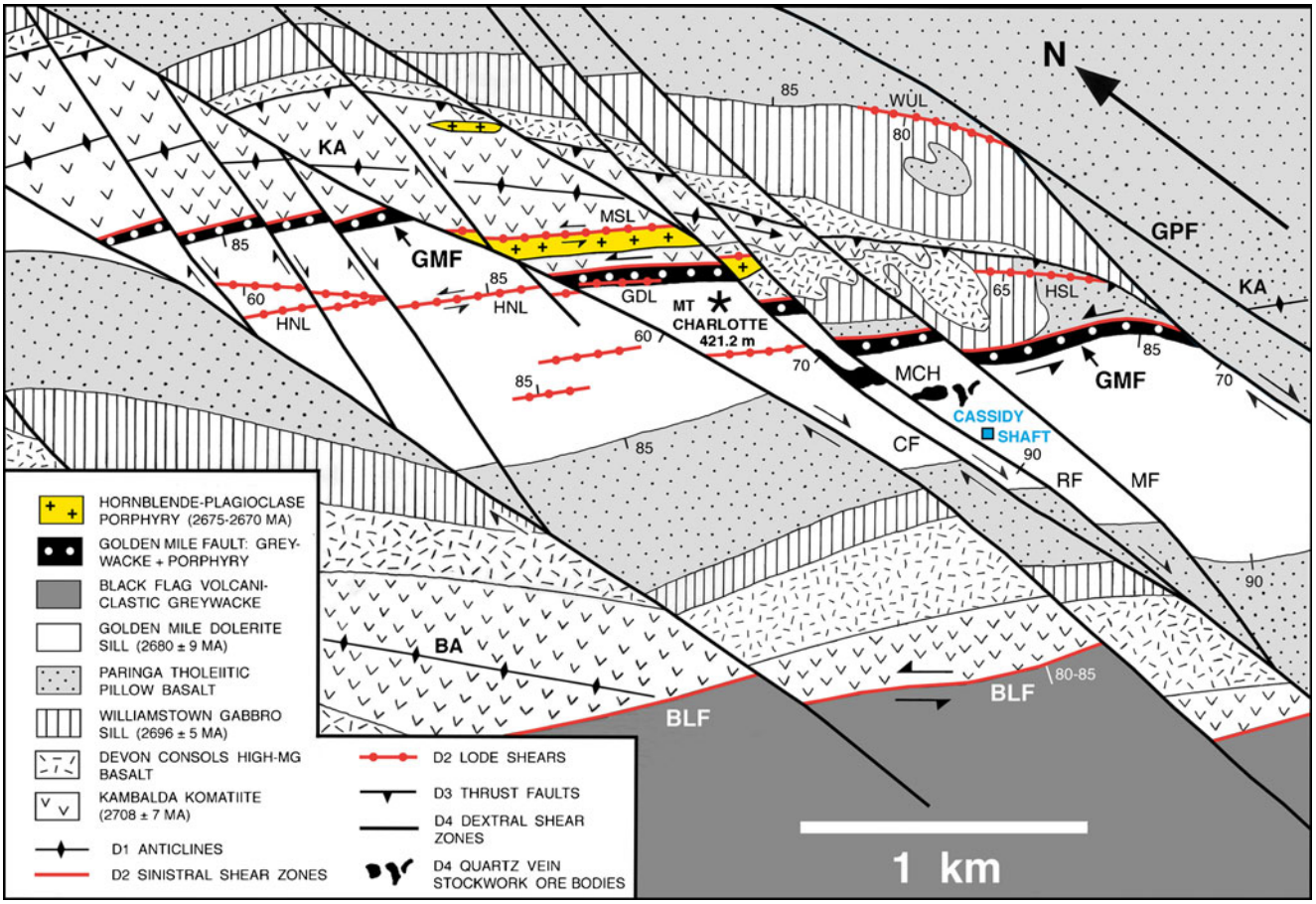

Fig. 2 Structural map of the Mt Charlotte area, northwest Kalgoorlie district (modified from Mueller et al. 1988). The Boulder and Kalgoorlie anticlines (*BA*, *KA*) are offset by the Golden Mile (*GMF*) and Boulder-Lefroy (*BLF*) strike-slip faults. The Hannan's North (*HNL*), Mystery (*MSL*), Golden Dream (*GDL*), Hidden Secret (*HSL*), and Westralia United lodes (*WUL*) are telluride-bearing D2 shear zones distal to the Golden Mile. The D4 quartz vein orebodies of the Mt Charlotte mine (*MCH*) are located between the Charlotte (*CF*), Reward (*RF*), and Maritana (*MF*) dextral strike-slip faults

The D3 thrusts are in turn displaced by north-striking dextral strike-slip faults (D4). The Golden Pike Fault has an offset of more than 2 km and separates the Mt Charlotte area from the Golden Mile. In the Mt Charlotte Mine, the D4 faults are closely spaced, dip 70–90° west, and control quartz vein stockworks preferentially developed in the granophyric unit 8 of the GMD. Pyrite and gold are disseminated in the inner sericite–ankerite replacement selvages of the veins, which grade outward into pervasive chlorite–dolomite–calcite alteration (Clout et al. 1990). The main Charlotte orebody, located between the Charlotte and Reward faults (Fig. 2), has horizontal dimensions of up to 75×250 m and has been mined from the surface to 950 m below datum. The smaller Reward orebodies are located between the Reward and Maritana faults. Total ore production amounts to 37 Mt at 3.4 g/t Au (1893–2001). The Charlotte gold–quartz veins are dated at 2,655±13 Ma (Pb–Pb xenotime; Rasmussen et al. 2009).

Field and analytical methods

In 1985–1987, underground mapping and sampling was carried out on the Cassidy shaft 22 level of the Mt Charlotte Mine and on several levels of the Paringa South and Lake View Main shafts in the Golden Mile (Mueller 1990). Composite mill heads of sulfide ore were prepared from the monthly period samples of the Fimiston mill. Channel samples taken across quartz veins of the Charlotte orebody in all drives on levels 19, 22, and 24 of the Cassidy shaft were combined into a single bulk sample. Trace element data and the analytical methods are listed in Table 1. Sample numbers refer to the museum collection of the University of Western Australia.

Twenty thin and polished sections from hand specimens taken on the Cassidy shaft 22 level were examined in transmitted and reflected light. Transparent minerals were identified according to optical properties

Table 1 Trace element composition of Golden Mile-type gold-telluride veins and replacement lodes (D2, D3) and of the younger Charlotte quartz vein orebody (D4), Kalgoorlie district, Western Australia

Structure	D4 stockwork	D2 shear zone	D2 shear zone	D3 shear zone	D2 shear zone	D2 shear zone	D2 shear zone	D2 shear zone
Gold stage	Early pyrite	Early pyrite	Early pyrite	Late telluride	Late telluride	Early py+po	Early py+po	Early py+po
Mine	Mt Charlotte	Lake View	Paringa	Paringa	Mt Charlotte	Mt Charlotte	Mt Charlotte	Mt Charlotte
Shaft	Cassidy	Lake View Main	Paringa South	Paringa South	Cassidy	Cassidy	Cassidy	Cassidy
Level	19, 22, 24	3–16	4	3	22	22	22	22
Host rock	GMD gabbro	GMD gabbro	GMD gabbro	Paringa Basalt	Greywacke	GMD gabbro	GMD gabbro	GMD gabbro
Sample	Bulk channel	210,410 tons ore	Kelly Lode	Oroya Shoot	Quartz vein	0.1 m from vein	0.5 m from vein	1 m from vein
UWA no.	109762	109738	109706	101921–23	109753	109756	109759	109757
Au (ppm)	2.73	7.00	3.62	556.00	23.00	0.59	0.80	0.48
Ag	0.80	3.40	5.00	81.00	172.00	1.60	0.50	0.20
Hg	0.06	3.13	4.26	98.00	8.00	0.05	n.a.	0.03
Bi	<0.1	<0.01	<0.1	0.30	1.57	0.20	<0.01	< 0.1
Cu	27	74	87	204	49	84	38	60
Pb	19	16	4	86	182	99	12	7
Zn	91	115	23	651	74	75	80	78
W	124	60	16	41	17,784	50	54	46
As	29.0	174.0	58.0	328.0	46.0	19.0	20.0	93.0
Sb	< 2	23.0	8.8	11.0	95.3	12.3	7.5	6.7
Te	1.0	9.4	15	871.0	134.8	2.0	0.5	< 1
Au/Ag	3.41	2.06	0.72	6.86	0.13	0.37	1.60	2.40
As/Sb	20.00	7.57	6.59	29.82	0.48	1.54	2.67	13.88

The large-tonnage ore sample from the Lake View mine represents the mill head of a half-year production period in 1985 at the Fimiston mill. The Mt Charlotte bulk sample represents the combined channel samples taken in all drives of the Charlotte orebody on three mine levels

Methods: Au by fire assay 25 g charge or by aqua regia digest 10 g charge (nos. 109753–109759; detection limit=0.01 ppm); Ag by mixed acid digest 0.5 g charge (DL=0.1 ppm); As, Cu, Pb, Zn, and W by X-ray fluorescence (XRF) pressed powder pellet (DL=1–7 ppm); Bi, Sb, and Te by inductively coupled plasma mass spectrometry (DL=0.01–0.1 ppm); Hg by cold vapor atomic absorption spectrometry; XRF analyses by XARL, University of Western Australia (all others by Genalysis Laboratory Services, Perth, Australia)

py pyrite, *po* pyrrhotite, *UWA no.* University of Western Australia, Department of Geology, museum specimen number (Mueller 1990)

tabled in Tröger (1971) and opaque minerals according to properties in Spry and Gedlinske (1987). A polished mount containing 140 handpicked grains of pyrite, gold, telluride, and sulfosalt was prepared from the non-magnetic fraction separated in heavy liquid from vein material (sample 109753). The separated and other in situ grains were analyzed at the Centre for Microscopy, Characterisation and Analysis at the University of Western Australia using a five-spectrometer JEOL JXA-8530F Hyperprobe operated at 20 kV and 20 nA. Calibration standards included pure metals for Ag, Au, Bi, Co, Cu, Fe, Ni, Se, and Sb and natural arsenopyrite, pyrite, altaite, and cinnabar. The analytical lines were S Kα, Fe Kα, Co Kα, Ni Kα, Cu Kα, As Lα, Se Lα, Ag Lα, Sb Lα, Te Lα, Au Mα, Hg Mα, Pb Mα, and Bi Mα. Counting times were 20 s on peaks and 10 s on the upper and lower backgrounds, resulting in low detection limits (0.01–0.03 wt%). Interference correction factors were calculated from the standards using proprietary JEOL software.

D2 and D3 lodes in the Golden Mile

Most of the D2 lodes forming the vast array of mineralized shear zones in Golden Mile Dolerite on both sides of the Golden Mile Fault were stoped underground over widths of 0.5–2.0 m, yielding sulfide ore with an average recovered grade of 11.3 g/t gold. Stopes at shear zone intersections were up to 10 m wide (Travis et al. 1971). A typical D2 lode consists of a major fault plane defining the footwall contact and of subsidiary fractures extending into its hanging wall, all filled with quartz–dolomite–calcite veins. The veins display heterogranular, breccia, banded, or crack-seal texture and, locally, cockade texture in breccia parts. Early-stage gold mineralization is associated with fine-grained pyrite in "bleached" sericite–ankerite selvages replacing chloritic GMD adjacent to the veins (Fig. 3a). The selvages coalesce where the altered shear zone becomes a "lode" (Fig. 3b) averaging 5–10 % disseminated pyrite. Most pyrite is arsenical (0.1–10 % As) and contains inclusions of chalcopyrite (Fig. 3c), tetrahedrite–tennantite, and native gold (1–15 μm)

constituting about 80 % of the gold budget (Travis et al. 1971). Oxidized assemblages such as magnetite+pyrite, hematite+magnetite+pyrite, and anhydrite+pyrite occur in parts of both lode systems (Stillwell 1931; Golding 1978; Mueller 2007). The early-stage pyrite mineralization, grading less than the average 11.3 g/t gold, is represented by the large-tonnage mill head sample from the Lake View Main shaft characterized by Au/Ag=2.1 and by As/Sb=7.6. Trace amounts of tellurides, in particular coloradoite (HgTe) and calaverite ($AuTe_2$), are always present, leading to elevated mercury and tellurium (Table 1). The high As/Sb ratio reflects the enrichment of arsenic in all lodes of the Golden Mile (Travis et al. 1971). The compilation of available Au/Ag ratios (Table 2) reveals large local variations (0.43–6.42). The low ratios (0.43–0.72) in the Paringa B Lode and Kelly Lode have not been linked to any early-stage silver mineral, yet.

Tellurides overprint the early pyrite and fill late tension gashes. They occur throughout the Golden Mile, account for about 20 % of the total gold, and characterize the high-grade ore shoots (>30 g/t Au) in both the D2 lodes and the D3 Oroya system (Travis et al. 1971; Golding 1978). Telluride-rich ore was most abundant in the upper 300 m of the deposit, as evidenced by underground production grades declining with time and depth (Woodall 1965). Nineteen tellurium-bearing minerals, commonly associated with late pyrite, chalcopyrite, tennantite–tetrahedrite, sphalerite, and native gold (898–972 fine), have been identified (Markham 1960; Golding 1978; Shackleton et al. 2003). Coloradoite is the most abundant and widespread telluride, accompanied by lesser altaite (PbTe) and rare melonite ($NiTe_2$), frohbergite ($FeTe_2$), tellurantimony (Sb_2Te_3), and native tellurium. Among the precious metal tellurides, calaverite and petzite (Ag_3AuTe_2) are abundant; krennerite ($Au_{1-X}Ag_XTe_2$), sylvanite [$(Ag,Au)_2Te_4$], and hessite (Ag_2Te) are minor; and montbrayite [$(Au, Sb)_2Te_3$] and nagyagite [$Pb_5Au(Te, Sb)_4S_{5-8}$] are rare. The assemblage native gold+calaverite±petzite (Fig. 3d) is earlier and far more common than the silver-rich assemblage hessite+petzite+sylvanite (Shackleton et al. 2003). Rare stibnite and Pb–Sb sulfosalts occur together with tellurides in lodes close to the Golden Mile Fault (Stillwell 1931). The sulfosalts include members of the bournonite ($CuPbSbS_3$)–seligmannite ($CuPbAsS_3$) series, boulangerite ($Pb_5Sb_4S_{11}$), and jamesonite ($Pb_4FeSb_6S_{14}$).

The average Au/Ag ratio of late-stage high-grade telluride ore is represented by three large-tonnage mill head samples (1900–1902) from the Kalgurli and Great Boulder Mines (range=1.37–3.56, average=2.54). Bulk samples (5–50 kg) and hand specimens (n=14) taken in individual lodes record a greater variation (range=0.87–16.00, average=5.02) but, with one exception, have ratios of >1 (Table 2). The D3 lodes of the reverse Oroya shear system are particularly enriched in gold (Au/Ag=3.15–16.00) and display high As/Sb and an elevated base metal content (Table 1). The As/Sb ratios of other lodes are >2.6 (Golding 1978).

D2 lodes in the Mt Charlotte area

Early-stage gold–pyrite ore from the Hannan's North Lode (Fig. 2) has Au/Ag=2.44, As/Sb=8.46, and a low tellurium content (8.3 ppm; Golding 1978), almost identical to the signature of low-grade ore in the Golden Mile (Tables 1 and 2). Late-stage tennantite, hessite, and melonite occur in the Mystery Lode (Sund et al. 1984), but the Hidden Secret (Fig. 2) remains the only telluride-rich D2 lode subject to microscopic study (Simpson 1912; Stillwell 1931). The ore consisted of early pyrite (up to 43 vol%); of late-stage twinned hessite and native gold; and of minor late-stage petzite, sylvanite, altaite, coloradoite, melonite, chalcopyrite, tetrahedrite–tennantite, and galena. Trace tetradymite (Bi_2Te_2S) and aguilarite (?) occurred enclosed in petzite and altaite, respectively. Contact assemblages include hessite–gold, hessite–galena, hessite–altaite, hessite–coloradoite, hessite–petzite, and hessite–sylvanite–petzite. Calaverite and krennerite are absent. The Au/Ag ratios (0.12–0.35) are far lower than those of any high-grade ore from the Golden Mile (Table 2).

D2 lodes, Mt Charlotte Mine 22 level

Golden Mile-type D2 lodes occur in Black Flag greywacke on the Cassidy shaft 22 level in a 15-m-long crosscut opened for a ventilation raise (Fig. 4). They are part of the Golden Mile Fault, which extends across the greywacke wedge (Feldtmann 1916; Clark 1980). The greywacke succession is overturned and composed of black carbonaceous siltstone and chert intercalated with graded beds of conglomeratic sandstone (Fig. 5a), all extensively replaced by hydrothermal sericite, Fe–dolomite, and minor calcite. Rounded detrital grains of quartz and thin carbonaceous beds are preserved even where alteration is intense. The beds are crossed by an offset dyke of GMD, which is moderately foliated and pervasively altered to fine-grained sericite+ankerite+quartz+albite. Chlorite+dolomite and remnant variolitic texture (Fig. 5b), characteristic of the unit 10 margin of the main sill (Travis et al. 1971), are preserved at the lower intrusive contact of the dyke. Sheared grains of igneous quartz (1–3 vol%) and meshwork rutile (0.5–1 mm) after titanomagnetite (2 vol%) also indicate offset from GMD units 9/10.

The Golden Mile Fault is represented by a system of narrow D2 shear zones which displace the mafic dyke in a sinistral sense, but are in turn offset by a barren D3 thrust subparallel in strike to the Flanagan Fault (Fig. 4b). The D2

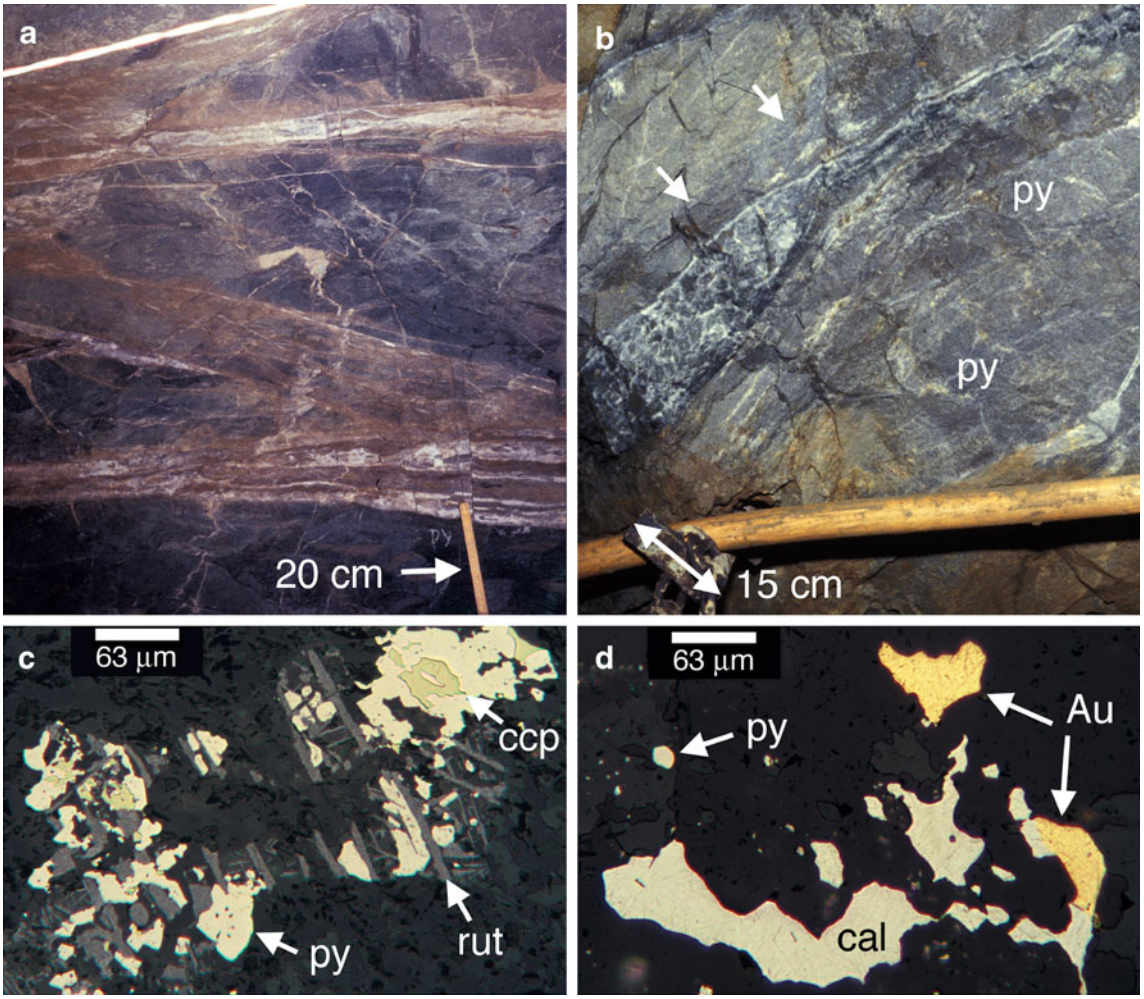

Fig. 3 Photographs of Golden Mile D2 lodes and reflected-light photomicrographs of early pyrite and late telluride mineralization. **a** Looking northeast at quartz–carbonate shear veins and tarnished sericite–ankerite–pyrite selvages (*brown*) of the Kelly Lode replacing dark green chloritic Golden Mile Dolerite. Paringa South shaft 4 level. **b** Looking south at a quartz–carbonate breccia vein of the Lake View Lode in sericite–ankerite altered Golden Mile Dolerite. Note the darker selvage (*arrows*) of fine-grained disseminated pyrite (*py*). Lake View Main shaft, 3 level south drive. **c** Kelly Lode: early-stage pyrite (*py*) and chalcopyrite (*ccp*) replace meshwork rutile (*rut*) pseudomorph after titanomagnetite. Paringa South shaft 4 level. **d** Oroya Hanging Wall Lode: late-stage calaverite (*cal*), native gold (*Au*), and pyrite (*py*) in quartz–carbonate gangue. Paringa South shaft 7 level

shear zones are filled with crack-seal veins in the dyke and with pinch-and-swell veins in greywacke (Fig. 5c, d). The crack-seal structure is defined by ribbons of comb quartz (2–10 mm), partly recrystallized to a granular mosaic, by laminae of sericite and rutile and by thin ribbons of carbonate and/or albite (Fig. 5e). The pinch-and-swell vein (Te vein in Fig. 4b) is subparallel to a bed of carbonaceous siltstone and is associated with gray chert-like replacement quartz brecciated and cemented by later quartz–dolomite–calcite fill (Fig. 5f).

Sulfide–telluride mineralization

Early-stage disseminated sulfides (0.5–0.8 g/t Au) occur in the altered GMD dyke between the veins in a zone more than 6 m wide and comprise pyrrhotite+pyrite (1–5 vol%), trace chalcopyrite, arsenopyrite, and, close to the veins, sphalerite and galena. Pyrrhotite increases in abundance away from the veins, forms anhedral aggregates and hexagonal crystals (Fig. 6a), and varies from non-magnetic to magnetic. The sulfides display zoned Au/Ag and As/Sb ratios, which decrease systematically toward the veins while lead, bismuth, and tellurium increase (Table 1).

The crack-seal veins in the GMD dyke contain aggregates of blue fluorescent scheelite, pyrite, minor chalcopyrite, and rare pyrrhotite and sphalerite. Late-stage tellurides were detected in a high-grade (23 g/t Au) pinch-and-swell vein in greywacke enriched in tellurium, silver, lead, bismuth, and mercury and characterized by particularly low Au/Ag and As/Sb ratios (Table 1). The narrow vein (Fig. 5d)

Table 2 Precious metal grades and Au/Ag of Golden Mile-type D2 and D3 lodes, Kalgoorlie district

Mine/orebody	Sample, vertical depth	Gold (g/t)	Silver (g/t)	Au/Ag ratio	Mineralization stage	Reference
Mount Charlotte area, NW end of Golden Mile system						
Hannan's North Lode	Bulk sample, 37.8 m	8.30	3.40	2.44	Early pyrite	Golding (1978)
Mt Charlotte Mine	Three blocks, 22 level	0.62	0.77	0.81	Early py+po	This study
Mt Charlotte Mine	Single block, 22 level	23.00	172.00	0.13	Late telluride	This study
Hidden Secret Lode	10,815 t ore to 1916	44.25	124.76	0.35	Late telluride	Feldtmann (1916)
Hidden Secret Lode	Single block, 61 m	602.30	5064.80	0.12	Late telluride	Simpson (1912)
Golden Mile: Eastern Lode System						
Lake View Mine	210,410 t ore 1985	7.00	3.40	2.06	Early pyrite	This study
Lake View Mine	Single block, 579 m	5.55	4.40	1.26	Early pyrite	Simpson (1912)
Lake View Lode	Single block, 10 level	11.00	3.80	2.89	Early pyrite	Golding (1978)
Associated mine	Single block, 555 m	8.93	9.44	0.95	Early pyrite	Simpson (1912)
Paringa B lode	Single block, 6 level	4.74	11.00	0.43	Early pyrite	This study
Paringa Kelly Lode	Bulk sample, 4 level	3.62	5.00	0.72	Early pyrite	This study
Kalgurli Mine	Av. ore July 1900	49.11	13.78	3.56	Late telluride	Simpson (1912)
Kalgurli Mine	Av. ore July 1902	31.31	11.61	2.70	Late telluride	Simpson (1912)
Lake View Lode	Single block, 91.4 m	294.96	195.03	1.51	Late telluride	Simpson (1912)
Brownhill Mine	Single block	51.66	25.00	2.07	Late telluride	Simpson (1912)
Blatchford Lode	Three blocks, 11 level	120.00	32.00	3.75	Late telluride	This study
Oroya HW Lode	Bulk sample, 7 level	48.00	3.00	16.00	Late telluride	This study
Oroya Shoot	Three blocks, 3 level	556.00	81.00	6.86	Late telluride	This study
Oroya Shoot	Bulk sample, 167.6 m	114.80	18.18	6.32	Late telluride	Simpson (1912)
Oroya Shoot	Single block, 250 m	43.11	4.85	8.89	Late telluride	Simpson (1912)
Oroya Shoot	Single block, 250 m	50.70	16.07	3.15	Late telluride	Simpson (1912)
Oroya Shoot	Single block, 555 m	775.26	79.97	9.69	Late telluride	Simpson (1912)
Golden Mile: Western Lode System						
No. 4 Lode, Chaffer's	Bulk drill core, 1384 m	4.00	2.70	1.48	Early pyrite	Golding (1978)
No. 4 Lode, Horseshoe	Bulk sample, 9 level	3.40	0.53	6.42	Early pyrite	Golding (1978)
Great Boulder Mine	105,802 t ore 1902	39.80	29.08	1.37	Late telluride	Simpson (1912)
No. 4 Lode, Boulder	Single block, 670.6 m	33.80	24.49	1.38	Late telluride	Simpson (1912)
No. 4 Lode, Boulder	Single block, 670.6 m	68.88	79.46	0.87	Late telluride	Simpson (1912)
Chaffer's East Lode	Bulk sample	180.29	32.46	5.55	Late telluride	Simpson (1912)
Chaffer's East Lode	Bulk sample	139.99	67.47	2.07	Late telluride	Simpson (1912)
Ivanhoe Mine	Single block, 307.8 m	20.47	9.57	2.14	Late telluride	Simpson (1912)

The Oroya lodes are D3 (reverse shear system); all others are D2 (sinistral shear system). Golden Mile mines are keyed to their lease or shaft names and worked several lodes. Depth below the surface is provided where reported. The standard vertical distance between mine levels is 100 ft (30.5 m)

Early py±po, <11.3 g/t Au (average underground); late telluride, >20–30 g/t Au

py pyrite, *po* pyrrhotite

was sampled because of abundant scheelite visible under ultraviolet light. Fine-grained subhedral pyrite of low arsenic (<0.21 %) and variable gold content (<0.03–0.10 %) is the dominant sulfide. The pyrite is in mutual contact with minor pyrrhotite, boulangerite (Fig. 6b, c), and bournonite. Both boulangerite ($Pb_5Sb_4S_{11}$) and bournonite ($CuPbSbS_3$) contain tellurium, indicating co-crystallization with telluride (Table 3). A single grain of silver-rich Pb–Sb sulfide (7.80 wt% Ag, 1.87 % Fe, 91.16 % total) was detected, but decomposed under the electron beam of the microprobe. Native gold of low fineness (834–857) and low mercury is associated with abundant hessite and lesser altaite. Hessite contains trace gold and altaite contains a little silver and bismuth (Table 3). Coloradoite was not detected, but is a likely accessory given the enrichment of mercury.

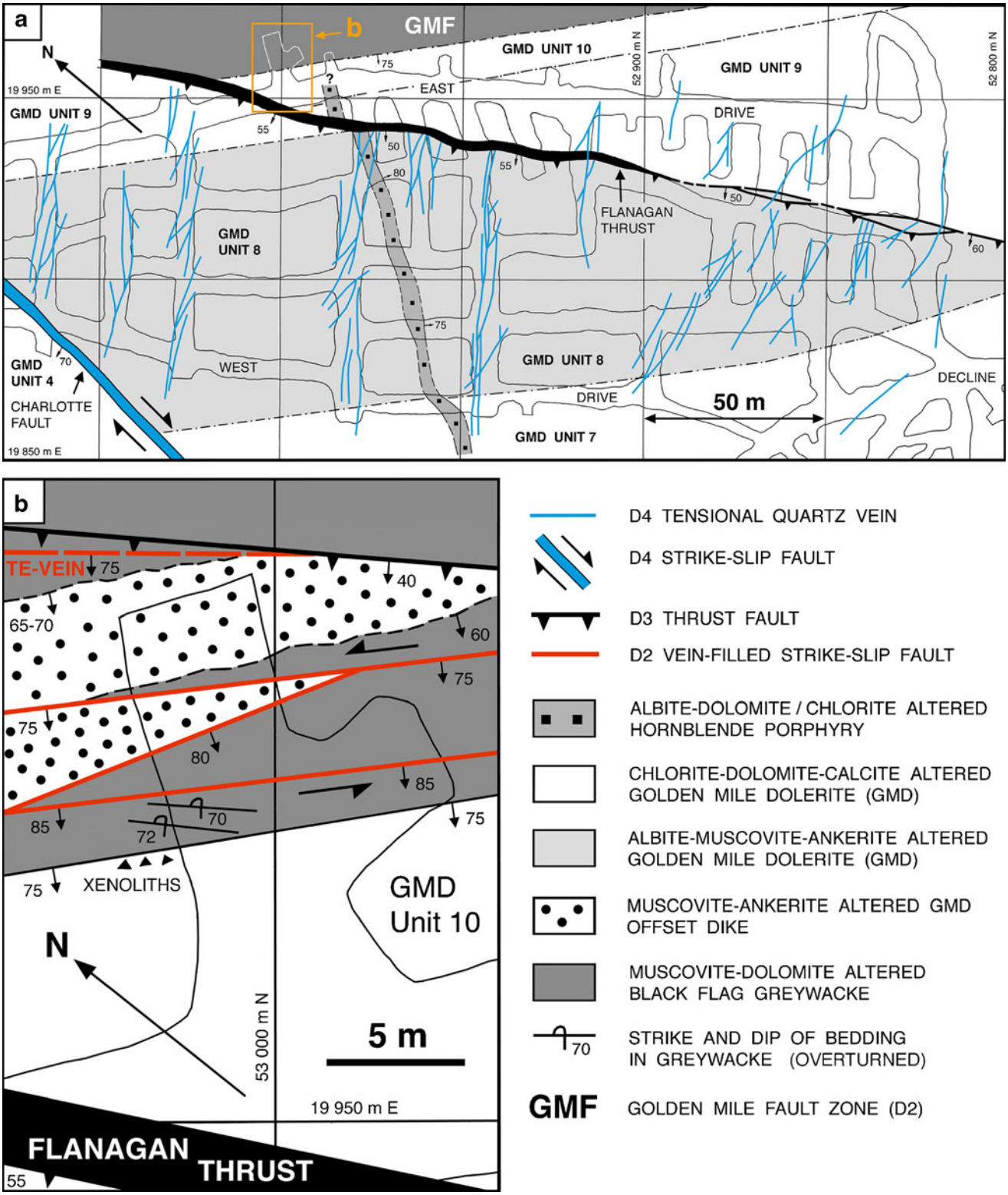

Fig. 4 Mineralized and barren structures on the Mt Charlotte mine 22 level (673 m below datum, 251.8 m below sea level) mapped in the backs of workings 4.5 m above the level. The coordinates are mine grid. **a** Plan section of the Charlotte quartz vein orebody. Sheared greywacke of the Kalgoorlie Syncline is part of the D2 Golden Mile Fault (*GMF*). The Golden Mile Dolerite (*GMD*) and a hornblende porphyry dyke are displaced by the D3 Flanagan thrust and by the D4 Charlotte strike-slip fault. Tensional quartz veins related to the Charlotte Fault are shown as mapped in the *crosscuts*. Note the location of Fig. 4b. **b** Structural map of the ventilation raise crosscut. Gold- and telluride-bearing D2 shear veins and a barren D3 thrust fault displace altered greywacke and a dyke offset from the main GMD sill. Sample 109753 is from the telluride-rich vein (Te vein) in greywacke; samples 109756–109759 represent altered mafic dyke (Table 1)

D4 quartz veins, Mt Charlotte Mine 22 level

On the Cassidy shaft 22 level (Fig. 4a), the quartz vein stockwork of the Charlotte orebody is limited by the D3 Flanagan thrust, which juxtaposes albite–sericite–ankerite altered GMD unit 8 in the hanging wall with chloritic quartz gabbro of units 9 and 10 in the footwall. Although tensional D4 quartz veins cut across the Flanagan Fault, they decrease in both thickness and abundance in unit 9, which does not attain bulk-minable gold grade. Most veins are oriented N55–65° E/60–90° NW and are zoned from quartz–albite or carbonate margins to inner massive quartz. Some contain central chlorite/calcite-lined vughs. The combined channel samples taken across veins of the Charlotte orebody on the 22 level, on the 19 level above, and on the 24 level below reveal low base metal but elevated tungsten contents, a signature similar to that of early-stage pyritic ore in the Golden Mile. Mercury and tellurium are much lower and the Au/Ag and As/Sb ratios are higher (Table 1).

Fig. 5 Photographs and photomicrographs of Black Flag greywacke, the Golden Mile Dolerite (*GMD*) offset dyke, and mineralized D2 shear veins, Mt Charlotte mine 22 level, ventilation raise crosscut (Fig. 4b). **a** Looking northwest at overturned graded beds of volcaniclastic greywacke containing nodules of diagenetic pyrite and fining upwards to the right, altered to sericite+carbonate. Note the thin beds of black carbonaceous siltstone. The scale is 43 cm. **b** GMD offset dyke: *left*, chlorite–dolomite rock from the lower margin preserving a variolitic texture defined by dolomite and epidote aggregates after igneous plagioclase (sample 109754); *right*, foliated sericite–ankerite rock containing disseminated pyrite (7 %) and pyrrhotite (5 %) between two scheelite-bearing quartz veins (sample 109755). The coin is 19 mm across. **c** Looking northwest at a crack-seal quartz–carbonate shear vein in sulfide-bearing sericite–ankerite altered GMD offset dyke (0.5–0.8 g/t Au). The scale is 1 m tall. **d** Looking northwest at the hessite-rich pinch-and-swell quartz–carbonate vein (23 g/t Au) in sericite–dolomite altered greywacke. The vein is displaced by a D3 thrust fault (*dashed line*). The scale is 1 m tall. **e** Crack-seal vein in GMD offset dyke: scheelite (*sch*) in contact with heterogranular quartz (*qtz*) and dolomite (*dol*). The adjacent quartz ribbon is comb-textured. The dolomite ribbon encloses minor sericite, opaque rutile, and quartz. Sample 109755, plane polarized light. **f** Hessite-rich vein in greywacke: chert-like replacement quartz (*qtz*) is crossed by carbonate veinlets, brecciated, and cemented by granoblastic dolomite+calcite (*cb*) containing opaque pyrite and interstitial aggregates of microcrystalline quartz. Sample 109753, crossed polarized light

Sulfide–telluride mineralization

The D4 quartz veins exposed on the 22 level contain blue fluorescent scheelite and pyrite, rare chalcopyrite, sphalerite, and native gold. Scheelite forms orange aggregates up to 10 cm long (Fig. 6d). The vein selvages in GMD unit 8 comprise an inner "bleached" albite–sericite–ankerite and an outer green chlorite–dolomite–calcite zone. Disseminated cube-shaped pyrite (10 vol%) in the inner gives way to magnetic fine-grained pyrrhotite (1–5 %) in the outer zone. Rare minerals enclosed in or attached to pyrite are native gold (Fig. 6e), chalcopyrite, and melonite (Fig. 6f). Melonite was identified (Table 3) in pyrite disseminated in the NE-striking dyke of hornblende porphyry (Fig. 4a). This dyke contains more nickel (107 ppm) than the adjacent GMD unit 8 (18 ppm). Rare grains of calaverite, krennerite, sylvanite, petzite, hessite, altaite, and tetrahedrite are reported to occur in other parts of the Charlotte orebody (Clout et al. 1990).

Discussion

The Golden Mile and Mt Charlotte at Kalgoorlie have been interpreted as "orogenic gold deposits" generated during fold-belt compression by metamorphic fluids ascending from the lower sialic crust (e.g., Groves et al. 1998, 2003; Goldfarb et al. 2005). Such deposits are expected to display rather uniform precious metal ratios of Au/Ag>5 and little or no zonation on the deposit scale. On the other hand, dykes of hornblende–plagioclase porphyry and lesser mica lamprophyre were emplaced into and adjacent to the Golden Mile Fault along the entire length of the district from 2,674±6 to 2,642±6 Ma, coincident with gold mineralization at ca. 2,655 or 2,645 Ma (McNaughton et al. 2005; Rasmussen et al. 2009; Vielreicher et al. 2010). These spatial and temporal relationships are more consistent with a magmatic–hydrothermal origin of the gold (Gustafson and Miller 1937; Mueller et al. 1988; Mueller 2007). Tellurides are particularly common in both liquid–magmatic and magmatic–hydrothermal ore deposits including komatiite-hosted Ni–Cu sulfide; norite-hosted Ni–Cu sulfide (e.g., Sudbury), skarns, greisens; and intrusion-related vein systems (Afifi et al. 1988a).

The recognition of kilometer-scale mineral and metal zonation has been a useful tool for targeted exploration within intrusion-centered mining districts. At Battle Mountain, Nevada, the precious metal ratio of Au–Ag–Cu deposits changes along the Virgin Fault south of the Copper Canyon granodiorite: Ag/Au=28–40 in garnet–pyroxene skarn (0- to 1,220-m distance), Ag/Au=19 in actinolite skarn (1,220–1,890 m), and Ag/Au=2 in distal chlorite–biotite replacement (1,890–2,400 m; Johnson 2000). In the Mankayan Cu–Au district, Philippines, the mercury and silver contents and the Ag/Au ratio of quartz–alunite alteration along the strike of the Lepanto Fault decrease systematically toward the Far Southeast porphyry deposit (1.42± 0.08 Ma). This pattern is disturbed by alteration zones related to the Guinaoang porphyry (3.5±0.5 Ma) in the southeast and by zones related to the Teresa veins (2.22± 0.05 Ma) in the south. Both are older and not part of the main system (Chang et al. 2011).

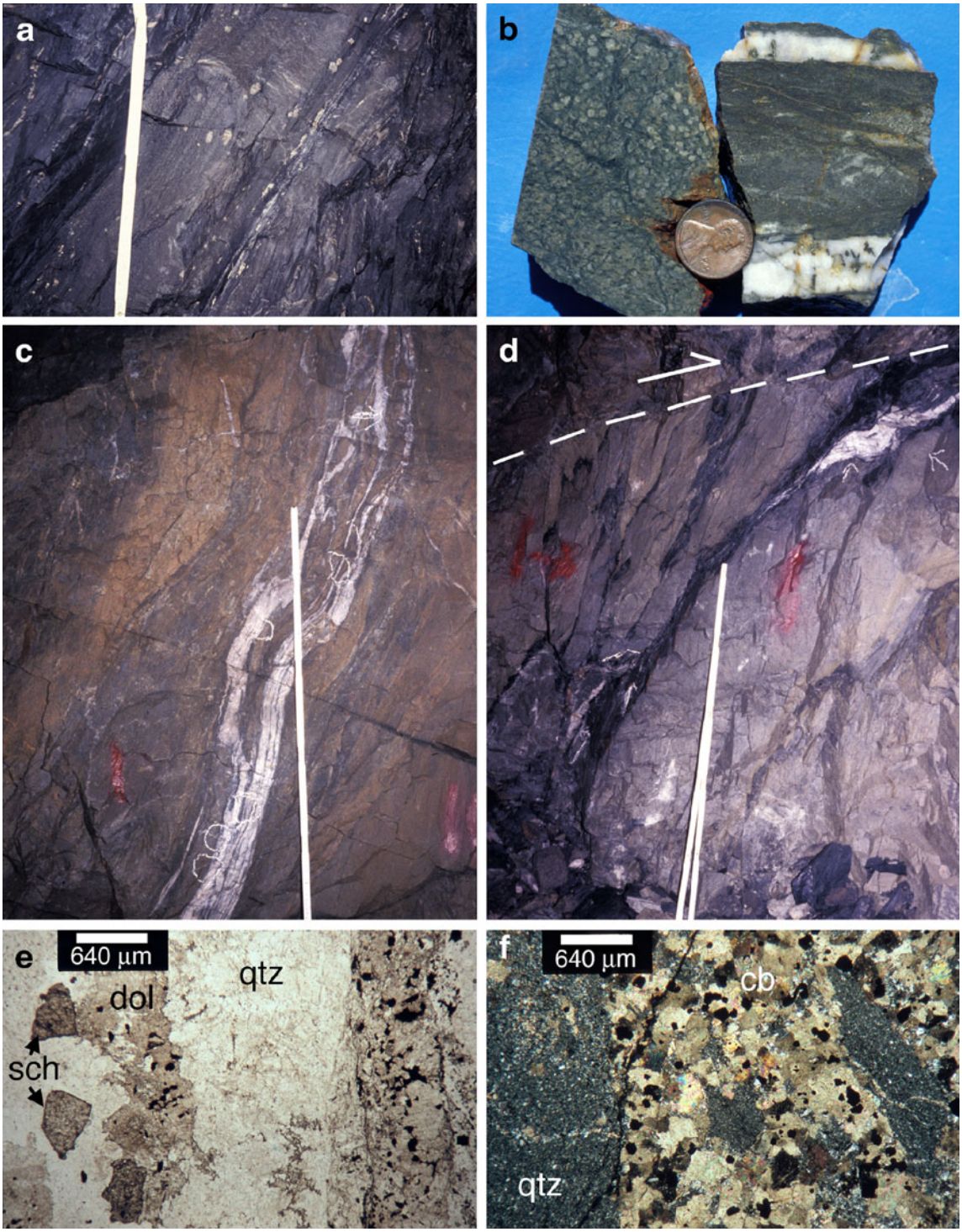

Timing of the Mt Charlotte quartz vein deposit

Structural mapping on the Mt Charlotte Mine 22 level establishes the relative time sequence for gold mineralization in the northwest Kalgoorlie district: Telluride-bearing D2 lodes are displaced by barren D3 thrust faults, which are in turn crosscut by D4 gold–quartz veins of the Charlotte orebody. Though the Mt Charlotte deposit is younger than the Golden Mile, the absolute age difference may be small, as discussed above with respect to the Mankayan district. The 2σ errors (±6–13 Ma) assigned to Archaean ages are too large to permit the necessary distinction. Apart from structure, there are geochemical and mineralogical differences, in particular the absence of hydrothermal magnetite+hematite±anhydrite and the scarcity of

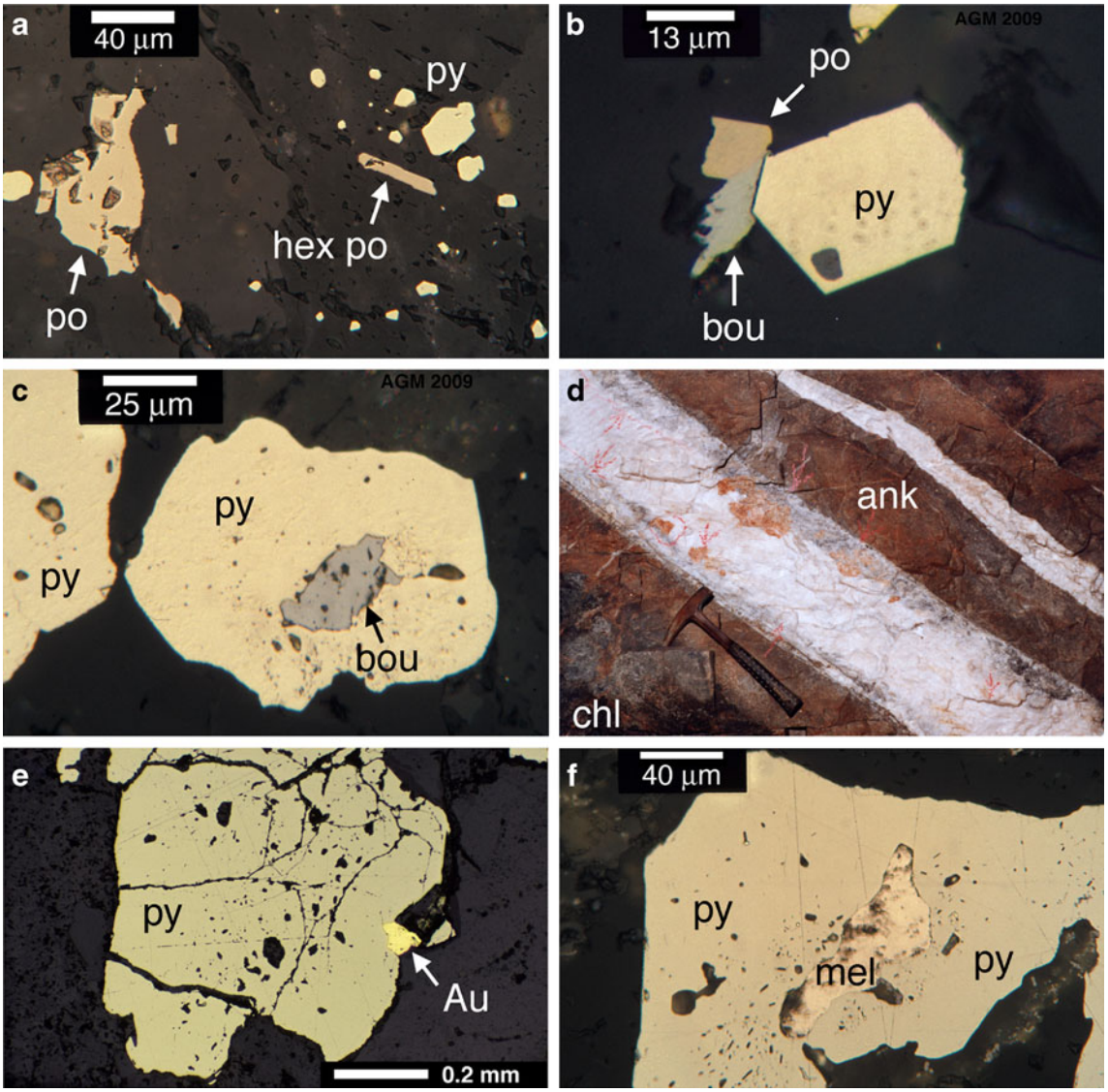

Fig. 6 Photographs and reflected-light photomicrographs of ore minerals in D2 and D4 veins and in the altered wall rocks, Mt Charlotte Mine 22 level. **a** D2 sulfides disseminated in the Golden Mile Dolerite (*GMD*) offset dyke: early-stage pyrite (*py*), tabular hexagonal pyrrhotite (*hex po*), and xenomorph magnetic pyrrhotite (*po*). Ventilation raise crosscut, sample 109755. **b** Hessite-rich D2 vein in greywacke: late-stage pyrite (*py*), pyrrhotite (*po*), and boulangerite (*bou*) in mutual contact. Ventilation raise crosscut, sample 109753. **c** Hessite-rich D2 vein in greywacke: late-stage boulangerite (*bou*) enclosed in pyrite (*py*). Ventilation raise crosscut, sample 109753. **d** D4 vein in GMD unit 8: orange scheelite in a tensional vein zoned from gray calcite–dolomite–quartz–albite margins to massive white quartz in the center. Pyrite-rich selvages of ankerite (*ank*)+albite± sericite are zoned to outer pyrrhotite-bearing chloritic alteration (*chl*). Western ore drive, close to the Charlotte Fault. The hammer is 33 cm long. **e** Ankerite–albite selvage of a D4 vein in GMD unit 8: native gold (*Au*) in mutual contact with pyrite (*py*). Central ore drive, sample 109745. **f** Albite–dolomite selvage of a D4 vein in porphyry: melonite (*mel*) enclosed in pyrite (*py*). Central ore drive, sample 109750

tellurides in the Charlotte orebody. Consequently, the Mt Charlotte deposit is excluded from the discussion of the Golden Mile system.

Metal zonation in the Golden Mile

The present data do not support metal zonation in early-stage gold–pyrite ore mined along the Golden Mile Fault. Pyritic ore from the Hannan's North Lode displays Au/Ag and As/Sb ratios very similar to those of low-grade ore from the Golden Mile. The wide pyrite–pyrrhotite zone of the D2 shear system on the Mt Charlotte Mine 22 level contrasts with the pyrite-only ore in the Golden Mile, but is considered to reflect the reducing nature of the local carbonaceous greywacke. The unusually low Au/Ag and As/Sb ratios of the altered wall rock are zoned relative to the D2 veins and are interpreted to relate to overprinting by late-stage sulfides. Ratios typical of Golden Mile sulfide ore are re-established at 1-m distance from the veins (Table 1).

Table 3 Electron microprobe analyses of pyrite, Pb–Sb sulfosalts, gold, and tellurides in the Golden Mile-type D2 shear vein (UWA no. 109753) and in the wall rock of tensional Charlotte D4 veins (UWA no. 109750), Mt Charlotte Mine 22 level, Kalgoorlie, Western Australia

Structure	Golden Mile-type D2 shear vein in sericite–dolomite altered Black Flag meta-greywacke														D4 vein
Mineral	Pyrite			Bournonite			Boulangerite		Gold			Hessite		Altaite	Melonite
No. of grains	1	1	9	1	1	1	1	5	1	1	6	1	7	1	1
Grain	pm-134	pm-100	All in pm	pm-29	pm-37	pts-6	pm-61	All in pts	pm-88	pm-38	All in pm	pm-78	All in pm	pm-124	pts29-1
No. analyses	1	1	9	3	3	1	3	5	1	1	6	1	7	1	1
Remarks	Min. As	Max. As	Mean	High Te	High Te	Low Te	Low Te	Mean	Min. Ag	Max. Ag	Mean	Max. Au	Mean	Low Bi	Low Sb
Fe (wt %)	46.80	46.64	46.81	<0.01	<0.01	0.04	<0.01	0.20	<0.01	<0.01	<0.01	<0.01	<0.01	<0.01	0.45
Ni	<0.01	<0.01	<0.01	<0.01	<0.01	<0.01	<0.01	<0.01	<0.01	<0.01	<0.01	<0.01	<0.01	0.01	18.96
As	<0.01	0.21	0.11	0.02	<0.01	0.10	<0.01	0.04	<0.01	<0.01	<0.01	<0.01	<0.01	<0.01	0.02
Sb	<0.01	<0.01	<0.01	25.04	24.91	24.80	26.16	25.79	<0.01	<0.01	<0.01	<0.01	<0.01	<0.01	0.71
Cu	0.02	<0.01	<0.01	12.66	12.67	12.98	<0.01	0.04	<0.01	0.04	0.02	<0.01	<0.01	0.01	<0.01
Pb	0.06	0.05	0.06	42.22	42.36	42.96	54.94	55.98	<0.03	<0.03	<0.03	<0.03	<0.03	61.22	<0.03
Bi	0.06	0.05	0.04	<0.03	0.06	n.a.	0.12	n.a.	<0.03	<0.03	<0.03	<0.03	<0.03	0.37	n.a.
Hg	<0.03	<0.03	<0.03	<0.03	<0.03	n.a.	<0.03	n.a.	0.71	0.76	0.68	<0.03	<0.03	<0.03	n.a.
Ag	<0.01	<0.01	<0.01	<0.01	<0.01	n.a.	<0.01	n.a.	14.34	16.60	15.52	63.20	62.64	0.16	n.a.
Au	<0.03	0.10	<0.03	<0.03	<0.03	n.a.	<0.03	n.a.	85.42	83.04	84.44	0.09	0.03	<0.03	n.a.
Te	<0.01	<0.01	<0.01	1.08	1.13	<0.01	0.11	0.06	<0.01	0.04	0.02	38.00	38.19	38.23	80.61
Se	<0.01	<0.01	<0.01	0.08	0.06	n.a.	0.06	n.a.	<0.02	<0.02	<0.02	<0.01	<0.01	<0.01	n.a.
S	53.75	53.49	53.78	18.87	18.79	19.24	18.08	18.37	<0.01	<0.01	<0.01	0.01	0.03	<0.01	0.07
Total	100.72	100.57	100.88	100.00	99.99	100.16	99.49	100.48	100.47	100.48	100.66	101.30	100.91	100.00	100.81
Norm atoms	3.000	3.000	3.000	6.000	6.000	6.000	20.000	20.000	1.000	1.000	1.000	3.000	3.000	2.000	3.000
Fe	0.999	0.999	0.999	0.000	0.000	0.004	0.000	0.067	0.000	0.000	0.000	0.000	0.000	0.000	0.025
Ni	0.000	0.000	0.000	0.000	0.000	0.000	0.000	0.000	0.000	0.000	0.000	0.000	0.000	0.000	0.998
As	0.000	0.003	0.002	0.001	0.001	0.006	0.001	0.011	0.000	0.000	0.000	0.000	0.000	0.000	0.000
Sb	0.000	0.000	0.000	1.022	1.019	1.003	4.105	3.995	0.000	0.000	0.000	0.000	0.000	0.000	0.018
Cu	0.000	0.000	0.000	0.990	0.993	1.006	0.000	0.012	0.000	0.001	0.000	0.000	0.000	0.000	0.000
Pb	0.000	0.000	0.000	1.013	1.018	1.021	5.068	5.097	0.000	0.000	0.000	0.000	0.000	0.988	0.000
Bi	0.000	0.000	0.000	0.000	0.001	0.000	0.011	0.000	0.000	0.000	0.000	0.000	0.000	0.006	0.000
Hg	0.000	0.000	0.000	0.000	0.000	0.000	0.000	0.000	0.006	0.007	0.006	0.000	0.000	0.000	0.000
Ag	0.000	0.000	0.000	0.000	0.000	0.000	0.001	0.000	0.233	0.266	0.250	1.986	1.977	0.005	0.000
Au	0.000	0.001	0.000	0.000	0.000	0.000	0.000	0.000	0.761	0.727	0.744	0.002	0.001	0.000	0.000
Te	0.000	0.000	0.000	0.042	0.044	0.000	0.016	0.008	0.000	0.000	0.000	1.010	1.019	1.001	1.953
Se	0.000	0.000	0.000	0.005	0.004	0.000	0.014	0.000	0.000	0.000	0.000	0.000	0.000	0.000	0.000
S	1.999	1.996	1.998	2.926	2.919	2.956	10.778	10.807	0.000	0.000	0.000	0.001	0.003	0.000	0.006

Label "pm" indicates grains in polished mount picked from the non-magnetic heavy liquid mineral fraction of 0.5 kg of vein material. Label "pts" indicates grains analyzed in situ in a polished thin section. Co is below detection (<0.02 %) in pyrite and in Pb–Sb sulfosalts

UWA no. University of Western Australia, Department of Geology, museum specimen number (Mueller 1990), *n.a.* not analyzed

In contrast, the occurrence of hessite-rich D2 veins on the Mt Charlotte Mine 22 level shows that the Hidden Secret Lode is not unique, indicating systematic changes in the mineralogy and precious metal content of late-stage gold–telluride ore along strike of the Golden Mile Fault. In the northwest (Mt Charlotte area): the absence of calaverite, gold of low fineness (834–857), hessite+altaite±petzite, low bulk Au/Ag (0.12–0.35), enrichment in lead. In the southeast (Golden Mile): gold of high fineness (898–972), calaverite+petzite±krennerite, high bulk Au/Ag (average=2.54, range=0.87–16.00), enrichment in copper and zinc. This zonation may be tested by the analysis of telluride-bearing drill core from the Mystery and other D2 lodes in the Mt Charlotte area and by analysis of drill core from the Paringa B Lode and Lake View Main Lode in the Golden Mile (Fig. 1).

Whether the kilometer-scale zonation in late-stage Au/Ag is accompanied by a zonation in late-stage As/Sb remains uncertain. The As/Sb ratio (0.48) of the Mt Charlotte telluride vein is drastically lower than the ratio (30) of the Oroya shoot, and stibnite and Pb–Sb sulfosalts are very rare in the Golden Mile. Antimonian montbrayite [$(Au, Sb)_2Te_3$] appears to be restricted to the margins of the western and eastern lode

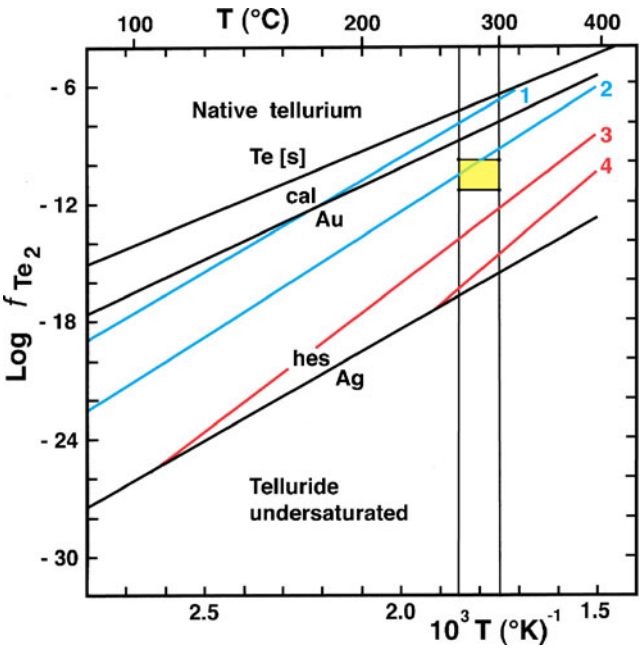

Fig. 7 Fugacity of Te_2–temperature diagram showing selected telluride reactions at different f_{S2} buffers within the boundaries set by tellurium condensation, gold–calaverite (*Au–cal*), and silver–hessite (*Ag–hes*) stability. Reactions: (*1*) galena–altaite at f_{S2}=magnetite–pyrite–hematite; (*2*) galena–altaite at f_{S2}=pyrrhotite–pyrite; (*3*) argentite–hessite at f_{S2}=magnetite–pyrite–hematite; (*4*) argentite–hessite at f_{S2}=pyrrhotite-pyrite (modified from Afifi et al. 1988a). The *vertical lines* indicate the temperature range (250–300 °C) of main telluride deposition in Golden Mile lodes. The *yellow field* outlines the fugacity calculated from the maximum–minimum silver contents of gold in the hessite-rich vein on the Mt Charlotte Mine 22 level. The field is drawn to overlap reaction *2*

systems (Golding 1978; Shackleton et al. 2003), providing some support for late antimony enrichment in the distal parts of the Golden Mile.

Constraints on Au–Ag telluride deposition

Shackleton et al. (2003) suggest that gold+calaverite+petzite and minor late hessite in the Golden Mile were deposited by a fluid cooling from 300 °C to below 170 °C, the lower temperature inferred from the decomposition of phases synthesized by Cabri (1965) to hessite+sylvanite and petzite+sylvanite. This interpretation implies a temperature control on the formation of hessite-rich D2 lodes.

Maximum fluid temperature

Chlorite and arsenopyrite thermometry constrain the temperature of early-stage gold–pyrite mineralization in Golden Mile D2 lodes to 340–390 °C (Bateman et al. 2001), an upper limit for telluride deposition in agreement with that imposed by the incongruent melting of krennerite (382±5 °C) and sylvanite (354±5 °C; Cabri 1965). In the Au–Ag–Te system, krennerite appears as an additional phase above about 280 °C, breaking the tie line calaverite–sylvanite (Afifi et al. 1988b). Late-stage veins and breccias in the Lake View Main Lode and in the Oroya Lodes contain inclusions of a low-salinity (≤5.5 wt% NaCl eq.) H_2O–CO_2 fluid trapped at temperatures of 290 and 250–315 °C, respectively (Ho et al. 1990). In this context, the fluid temperature of about 300 °C assumed by Shackleton et al. (2003) for the deposition of gold+calaverite+petzite±krennerite is reasonable, though a greater range of 290–340 °C is possible.

Minimum fluid temperature

A lower temperature limit for hydrothermal activity in the Kalgoorlie district, and thus for the deposition of silver-rich tellurides, is imposed indirectly by the trapping pressures of primary fluid inclusions in quartz, which are 280 MPa for the D2 Lake View Main Lode, 160–210 MPa for the D3 Oroya Lodes, and 150–300 MPa for the D4 tensional veins of the Charlotte orebody (Ho et al. 1990; Mernagh et al. 2004). In combination with the estimate of 400±150 MPa for the Hannan South Au–Cu skarn 12 km southeast of Kalgoorlie (Mueller et al. 2012), these data indicate a regional lithostatic pressure of 250–300 MPa during the formation of the Golden Mile deposit. Assuming 3.6 km per 100 MPa for the granite–greenstone terrane (Spear 1993), this converts to a burial depth of 9–11 km. Given a low geothermal gradient of 25 °C/km (Barton and Hanson 1989), the ambient temperature of the terrane is estimated at 250 °C, setting the lower limit any hydrothermal fluid could cool to.

Some of the hessite in the Golden Mile and in the Hidden Secret Lode occurs in micrographic intergrowth with sylvanite (Stillwell 1931) and probably formed below 170 °C by decomposition of a higher temperature phase, as deduced by Shackleton et al. (2003). However, this process took place during the uplift and slow cooling of the terrane long after hydrothermal activity had ceased.

Tellurium fugacity of the fluid

The temperature constraints outlined suggest a lateral gradient of about 50 °C during the main phase of telluride deposition in the Golden Mile hydrothermal system. This gradient, relatively small due to the burial depth of 10 km, suggests that fluid temperature was not the main cause of lateral mineral and Au–Ag zonation. The most likely cause is a decrease in the activity of tellurium stabilizing hessite relative to calaverite (Afifi et al. 1988a). In the central part of the Golden Mile system, a late input fluid of high tellurium fugacity overprinted the initial gold–pyrite mineralization in the wall rock. This fluid deposited minor solid or liquid tellurium by condensation and then abundant calaverite and high-fineness gold at conditions set by the calaverite–gold buffer (Fig. 7). With time, the tellurium fugacity declined, stabilizing hessite and low-fineness gold.

In the Mt Charlotte area at the periphery of the hydrothermal system, the late input fluid did not maintain the high tellurium fugacity required for the deposition of calaverite. The assemblage hessite–gold in the Mt Charlotte D2 vein allows the estimation of the local tellurium fugacity using Eq. 18 in Afifi et al. (1988b) based on the reaction:

$$4\,Ag + Te_2 = 2\,Ag_2Te$$

Unit activity for hessite is indicated by the mean of the microprobe analyses (Table 3). At 250–300 °C, the minimum silver content in gold (23.3 at.% Ag) gives log $f_{Te2} = -11.2$ to -9.8, and the maximum content (26.6 at.% Ag) gives log $f_{Te2} = -11.7$ to -10.2. The temperature–fugacity field of these data has to be extended across the altaite–galena reaction at the pyrite–pyrrhotite f_{S2} buffer (Fig. 7) to account for the presence of all four minerals in the Mt Charlotte D2 vein system. The contact assemblages gold–hessite, hessite–altaite, and hessite–galena in the nearby Hidden Secret Lode indicate a similar fugacity range, perhaps shifted to slightly higher log f_{Te2} given the absence of pyrrhotite.

Conclusions

The telluride-poor Mt Charlotte gold quartz vein deposit is structurally related to the youngest set (D4) of strike-slip faults in the Kalgoorlie district and represents a separate hydrothermal system, which did not contribute to the metal content of the older Golden Mile (D2). Low-grade pyritic replacement lodes in D2 shear zones (<11 g/t Au), most containing late high-grade gold–telluride shoots (>30 g/t Au), occur over a strike length of 8 km adjacent to the D2 Golden Mile Fault. In the northwest part of the district near Mt Charlotte, these telluride-rich shoots are characterized by low Au/Ag ratios (0.12–0.35) relative to those in the main part of the Golden Mile (Au/Ag=2.54) to the southeast. The silver-rich nature is related to the assemblages gold (834–857 fine)+hessite, hessite+altaite, and hessite+petzite± sylvanite. The earlier assemblage gold (898–972 fine)+calaverite+petzite±krennerite, predominant in the central Golden Mile, is absent in the northwest. The lateral transition from calaverite to hessite and the related change in the Au/Ag ratio of gold–telluride ore indicate kilometer-scale metal zonation within the mercury (coloradoite) footprint of the giant Golden Mile system. Another vector may be provided by the As/Sb ratio, which appears to be lower in distal (As/Sb=0.5) than in proximal telluride-rich ore (As/Sb>2.6).

The lateral Au–Ag zonation is attributed to a gradual decline in peak tellurium fugacity toward the distal parts of the hydrothermal system, which stabilized tellurium-poor hessite+gold at the periphery and tellurium-rich calaverite+gold in the center. A concomitant decline in fluid temperature from about 300 to 250 °C is possible. The deposition of sulfides preceded that of tellurides in all lodes, reflecting a late input of H_2Te relative to the input of sulfur from the same source (Afifi et al. 1988a), a sequence the Golden Mile shares with classic magmatic–hydrothermal vein systems such as Cripple Creek in Colorado (Lindgren 1933), El Indio-Tambo in Chile (Siddeley and Araneda 1986), and Acupan in the Philippines (Cooke et al. 1996).

Acknowledgments Andreas Mueller acknowledges receipt of a scholarship during his PhD study at the University of Western Australia (UWA) in 1985–1990. He is grateful to Jim Cleghorn, chief geologist of the former Kalgoorlie Mining Associates, who advised on Mt Charlotte geology and lent his valuable flashlight as an introduction to underground photography. Both authors acknowledge access to the Australian Microscopy and Microanalysis Research Facility at the Centre for Microscopy, Characterisation and Analysis (CMCA) funded by the university (UWA), State, and Commonwealth Governments. We thank Dr. Ray Chang, former XARL at UWA, and John Flynn at Genalysis Laboratory Services (Intertek) for sharing their expertise in chemistry.

References

Afifi AM, Kelley WC, Essene EJ (1988a) Phase relations among tellurides, sulfides, and oxides: II. Applications to telluride-bearing ore deposits. Econ Geol 83:395–404

Afifi AM, Kelley WC, Essene EJ (1988b) Phase relations among tellurides, sulfides, and oxides: I. Thermochemical data and calculated equilibria. Econ Geol 83:377–394

Barton MD, Hanson RB (1989) Magmatism and the development of low-pressure metamorphic belts: implications from the western United States and thermal modelling. Geol Soc Am Bull 101:1051–1065

Bateman RJ, Hagemann SG, McCuaig TC, Swager CP (2001) Protracted gold mineralization throughout Archaean orogenesis in the Kalgoorlie camp, Yilgarn Craton, Western Australia: structural, mineralogical, and geochemical evolution. Geological Survey of Western Australia, Record 2001/17, pp 63–98

Cabri LJ (1965) Phase relations in the Au–Ag–Te system and their mineralogical significance. Econ Geol 60:1569–1606

Cassidy KF, Champion DC, Krapez B, Barley ME, Brown SJA, Blewett RS, Groenewald PB, Tyler IM (2006) A revised geological framework for the Yilgarn Craton, Western Australia. Geological Survey of Western Australia, Record 2006/8, 8 pp

Chang Z, Hedenquist JW, White NC, Cooke DR, Roach M, Deyell CL, Garcia J Jr, Gemmell JB, McKnight S, Cuison AL (2011) Exploration tools for linked porphyry and epithermal deposits: example from the Mankayan intrusion-centered Cu–Au district, Luzon, Philippines. Econ Geol 106:1365–1398

Clark ME (1980) Localization of gold, Mt Charlotte, Kalgoorlie, Western Australia. BSc Honours thesis, University of Western Australia, Perth, 128 pp

Clout JMF, Cleghorn JH, Eaton PC (1990) Geology of the Kalgoorlie goldfield. In: Hughes FE (ed) Geology of the mineral deposits of Australia and Papua New Guinea. Australasian Inst Min Metall, Melbourne, Monograph 14, pp 411–431

Cooke DR, McPhail DC, Bloom MS (1996) Epithermal gold mineralization, Acupan, Baguio district, Philippines: geology, mineralization, alteration, and the thermochemical environment of ore deposition. Econ Geol 91:243–272

Feldtmann FR (1916) Contributions to the study of the geology and ore deposits of Kalgoorlie, East Coolgardie Goldfield, Part 3. Geol Survey Western Australia, Bulletin 69, 152 pp

Fletcher IR, Dunphy JM, Cassidy KF, Champion DC (2001) Compilation of SHRIMP U–Pb geochronological data, Yilgarn Craton, Western Australia, 2000–2001. Geoscience Australia, Record 2001/47, 111 pp

Goldfarb RJ, Baker T, Dubé B, Groves DI, Hart CJR, Gosselin P (2005) Distribution, character, and genesis of gold deposits in metamorphic terranes. Economic Geology 100th Anniversary Volume, pp 407–450

Golding LY (1978) Mineralogy, geochemistry and origin of the Kalgoorlie gold deposits, Western Australia. PhD thesis, University of Melbourne, 402 pp

Groves DI, Goldfarb RJ, Gebre-Mariam M, Hagemann SG, Robert F (1998) Orogenic gold deposits: a proposed classification in the context of their crustal distribution and relationship to other gold deposit types. Ore Geol Rev 13:7–27

Groves DI, Goldfarb RJ, Robert F, Hart CJR (2003) Gold deposits in metamorphic belts: overview of current understanding, outstanding problems, future research, and exploration significance. Econ Geol 98:1–29

Gustafson JK, Miller FS (1937) Kalgoorlie geology reinterpreted. Australas Inst Min Metall Proc 106:93–125

Ho SE, Bennett JM, Cassidy KF, Hronsky JMA, Mikucki EJ, Sang JH (1990) Fluid inclusion studies. In: Ho SE, Groves DI, Bennett JM (eds) Gold deposits of the Archaean Yilgarn Block, Western Australia: nature, genesis, and exploration guides. University of Western Australia, Publication 20, pp 198–211

Johnson TW (2000) Metal and mineral zoning at the Greater Midas Au–Cu–Ag skarn deposit (Battle Mountain district), Lander County, Nevada. In: Cluer JK, Price JG, Struhsacker EM, Hardyman RF, Morris CL (eds) Geology and ore deposits 2000: the Great Basin and beyond. Geol Soc Nevada Symposium Proceedings, 15–18 May 2000, pp 1083–1106

Keats W (1987) Regional geology of the Kalgoorlie–Boulder gold-mining district. Geol Survey Western Australia, Report 21, 44 pp

Kent AJR, McDougall I (1995) $^{40}Ar/^{39}Ar$ and U–Pb age constraints on the timing of gold mineralization in the Kalgoorlie goldfield, Western Australia. Econ Geol 90:845–859

Lindgren W (1933) Mineral deposits, 4th edn. McGraw-Hill, New York, 930 pp

Markham NL (1960) Synthetic and natural phases in the system Au–Ag–Te. Econ Geol 55:1148–1178, 1460–1477

McNaughton NJ, Mueller AG, Groves DI (2005) The age of the giant Golden Mile deposit, Kalgoorlie, Western Australia: ion-microprobe zircon and monazite U–Pb geochronology of a syn-mineralization lamprophyre dike. Econ Geol 100:1427–1440

Mernagh TP, Heinrich CA, Mikucki EJ (2004) Temperature gradients recorded by fluid inclusions and hydrothermal alteration at the Mount Charlotte gold deposit, Kalgoorlie, Australia. Can Mineral 42:1383–1403

Mueller AG (1990) The nature and genesis of high- and medium-temperature Archaean gold deposits in the Yilgarn Block, Western Australia, including a specific study of scheelite-bearing gold skarn deposits. PhD thesis, The University of Western Australia, Perth, 144 pp

Mueller AG (2007) Copper-gold endoskarns and high-Mg monzodiorite-tonalite intrusions at Mt. Shea, Kalgoorlie, Australia: implications for the origin of gold-pyrite-tennantite mineralization in the Golden Mile. Miner Depos 42:737–769

Mueller AG, McNaughton NJ (2000) U–Pb ages constraining batholith emplacement, contact metamorphism, and the formation of gold and W–Mo skarns in the Southern Cross area, Yilgarn Craton, Western Australia. Econ Geol 95:1231–1257

Mueller AG, Harris LB, Lungan A (1988) Structural control of greenstone-hosted gold mineralization by transcurrent shearing: a new interpretation of the Kalgoorlie mining district, Western Australia. Ore Geol Rev 3:359–387

Mueller AG, Lawrance LM, Muhling J, Pooley GD (2012) Mineralogy and PTX relations of the Archaean Hannan South Au–Cu (Co–Bi) deposit, Kalgoorlie, Western Australia: thermodynamic constraints on the formation of a zoned intrusion-related skarn. Econ Geol 107:1–24

Nelson DR (1997) Evolution of the Archaean granite–greenstone terranes of the Eastern Goldfields, Western Australia: SHRIMP U–Pb zircon constraints. Precambrian Res 83:57–81

Rasmussen B, Mueller AG, Fletcher IR (2009) Zirconolite and xenotime U–Pb constraints on the emplacement of the Golden Mile Dolerite sill and gold mineralization at the Mt Charlotte mine, Eastern Goldfields Province, Yilgarn Craton, Western Australia. Contr Mineral Petrol 157:559–572

Shackleton JM, Spry PG, Bateman R (2003) Telluride mineralogy of the Golden Mile deposit, Kalgoorlie, Western Australia. Can Mineral 41:1503–1524

Siddeley G, Araneda R (1986) The El Indio-Tambo gold deposits, Chile. In: Macdonald AJ (ed) Proceedings of Gold'86. Konsult International Inc., Willowdale, pp 445–456

Simpson ES (1912) Detailed mineralogy of Kalgoorlie and Boulder with special reference to the ore deposits. In: Simpson ES, Gibson CG (eds) The geology and ore deposits of Kalgoorlie, East Coolgardie Goldfield, part 1. Geological Survey of Western Australia, Bulletin 42, pp 77–151

Spear FS (1993) Metamorphic phase equilibria and pressure–temperature–time paths. Mineralogical Society of America Monograph 1, 799 pp

Spry PG, Gedlinske BL (1987) Tables for the determination of common opaque minerals. Economic Geology Publishing, Littleton, 52 pp

Squire RJ, Allen CM, Cas RAF, Campbell IH, Blewett RS, Nemchin AA (2010) Two cycles of voluminous pyroclastic volcanism and sedimentation related to episodic granite emplacement during the late Archaean: eastern Yilgarn Craton, Western Australia. Precambrian Res 183:251–274

Stillwell FL (1929) Geology and ore deposits of the Boulder Belt, Kalgoorlie. Geological Survey of Western Australia, Bulletin 94, 110 pp

Stillwell FL (1931) The occurrence of telluride minerals at Kalgoorlie. Proc Austr Inst Min Metall 84:115–190

Sund JO, Schwabe MR, Hamlyn DA, Bonsall EM (1984) Gold mineralization at the north end of the Kalgoorlie Field, Mount Percy–Kalgoorlie, Western Australia. Regional Conference on Gold Mining, Metallurgy and Geology, Geology Section, pp 1–8. Austr Inst Min Metall, Perth and Kalgoorlie Branches

Swager CP, Griffin TJ, Witt WK, Wyche S, Ahmat AL, Hunter WM, McGoldrick PJ (1995) Geology of the Archaean Kalgoorlie terrane—an explanatory note. Geol Survey Western Australia, Report 48, 26 pp

Travis GA, Woodall R, Bartram GD (1971) The geology of the Kalgoorlie Goldfield. In: Glover JE (ed) Symposium on Archaean Rocks. Geological Society of Australia, Special Publication 3, pp 175–190

Tröger WE (1971) Optische Bestimmung der gesteinsbildenden Minerale. Teil 1 Bestimmungstabellen, 4th edition. Schweizerbart'sche Verlagsbuchhandlung, Stuttgart, 188 pp

Vielreicher NM, Groves DI, Snee LW, Fletcher IR, McNaughton NJ (2010) Broad synchroneity of three gold mineralization styles in the Kalgoorlie Gold Field: SHRIMP U–Pb, and ^{40}Ar–^{39}Ar geochronological evidence. Econ Geol 105:187–227

Woodall RW (1965) Structure of the Kalgoorlie Goldfield. In: McAndrew J (ed) Geology of Australian ore deposits. Melbourne, 8th Commonwealth Min Metall Congress, pp 71–79